JOURNAL OF MATERIALS SCIENCE 31 (1996) 2957–2963

Effects of surface and sizing treatments on axial compressive strength of carbon fibres

M. MIWA, A. TAKENO, Y. MORI, T. YOKOI, A. WATANABE
Faculty of Engineering, Gifu University, Yanagido 1-1, Gifu, Japan 501-11

Attempts have been made to estimate the fibre axial compressive strength of pitch-based graphitized fibres, and the effects of surface- and size-treatment on compressive strength was investigated. The estimated compressive strength of fibres decreases with increasing temperature. This decrease in compressive strength may be accounted for by a decrease in the radial compression force owing to a decrease in the residual thermal stress and a decrease in Young's modulus of the resin matrix. There is a linear relationship between the estimated compressive strength and radial compression force in a temperature range from room temperature to 80 °C. The real compressive strength of the fibres, determined by extrapolating this straight line until the radial compression force is zero, increases with increasing shear yield strength at the fibre–matrix interphase. In order to obtain reinforcing fibres with a higher compressive strength, it will be necessary to surface- and size-treat the fibres.

1. Introduction

The relation between the mechanical properties of composites in tension and those of the fibres used as reinforcements have been studied both experimentally and theoretically in fairly great detail. However, in spite of the fact that the compressive characteristics of composites depend on the characteristics of reinforcing fibres, there is almost no study of the mechanical properties of composites in compression. Several efforts [1–5] to determine the compressive characteristics of reinforcing fibres have been made, but there is still no decisive method.

We have reported a method for measuring the compressive strength of fibres, i.e. if a sufficiently long fibre is embedded in the neighbourhood of the surface of a rectangular beam and the system is subjected to a tensile (or compressive) strain rather than a fibre ultimate strain, according to the bending method, the fibre eventually breaks into many pieces. By measuring the lengths of the broken pieces, the axial compressive strength of the fibre can be estimated in both cases where the tensile strength of the fibres is assumed to be uniform [6, 7] and where it is assumed to be variable [8, 9].

Using the latter method, we estimated the compressive strengths of carbon and aramid fibres. It was found that the estimated compressive strength of PAN-based carbon fibres was higher than pitch-based fibres, and that of carbonized fibres (higher strength type) was higher than graphitized fibres (higher modulus type) [6, 7, 9, 10]. Moreover, the axial fibre compressive strength was approximately 10–60% of the tensile strength [9]. It increased with increasing degree of orientation or face spacing of the crystal and increased with decreasing crystal size [10]. In addition, it increased with decreasing fibre diameter [11]. Furthermore, it was only 2–3% of the tensile strength for aramid fibres due to the formation of kink bands [8].

It is generally known that in order to improve the reinforcing efficiency, i.e. to improve the wettability at the fibre–matrix interface, the fibres are generally surface-treated and size-treated. However, there have been no studies of the effect of fibre surface and sizing treatments on the compressive strength of reinforcing fibres.

In this work, the effects of the fibre surface and sizing treatments on the compressive strength of carbon fibres was investigated using the method described elsewhere [7, 8] in which the tensile strength of the fibres was taken into consideration. Furthermore, we will give a guide to the development of the carbon fibres with higher axial compressive strength.

2. Experimental procedure

The fibres used were six kinds of pitch-based graphitized fibres (higher modulus type, experimental samples of Tonen) which were surface- and/or size-treated. Mechanical properties are shown in Table I.

First, tensile tests were performed using 5, 10, 15, 20, 25, 30, and 100 mm gauge lengths, respectively, to obtain distribution curves of the tensile strength of the fibres. The instrument used was a Tensilon UTM-I-2500 type (Orientec), strain rate 0.1 mm/mm/min, and the number of fibres tested was more than a hundred pieces for each gauge length. The results obtained by the fibre tensile strength distribution tests were used to determine Weibull parameters.

Second, rectangular specimens were prepared for measuring fragment length under the same conditions as reported in previous papers [6–11]. 100 parts of

0022–2461

TABLE I Mechanical properties of fibres with various surface- and/or sizing-treatments (at 20 °C)

Description	Surface treatment	Sizing treatment	Diameter (μm)	Tensile strength (GPa)	Young's modulus (GPa)	Breaking strain (%)
I	none	none	9.9	3.33	510	0.68
II	10	none	9.8	3.44	480	0.74
III	none	A	10.1	3.26	488	0.79
IV	10	A	9.9	3.38	498	0.73
V	none	B	9.9	3.39	505	0.67
VI	10	B	10.0	3.53	516	0.67

Surface treatment: 10 C cm^{-2}.
Sizing agent: A ethylene oxide; B epoxy oligomer.
Test length: 25 mm.

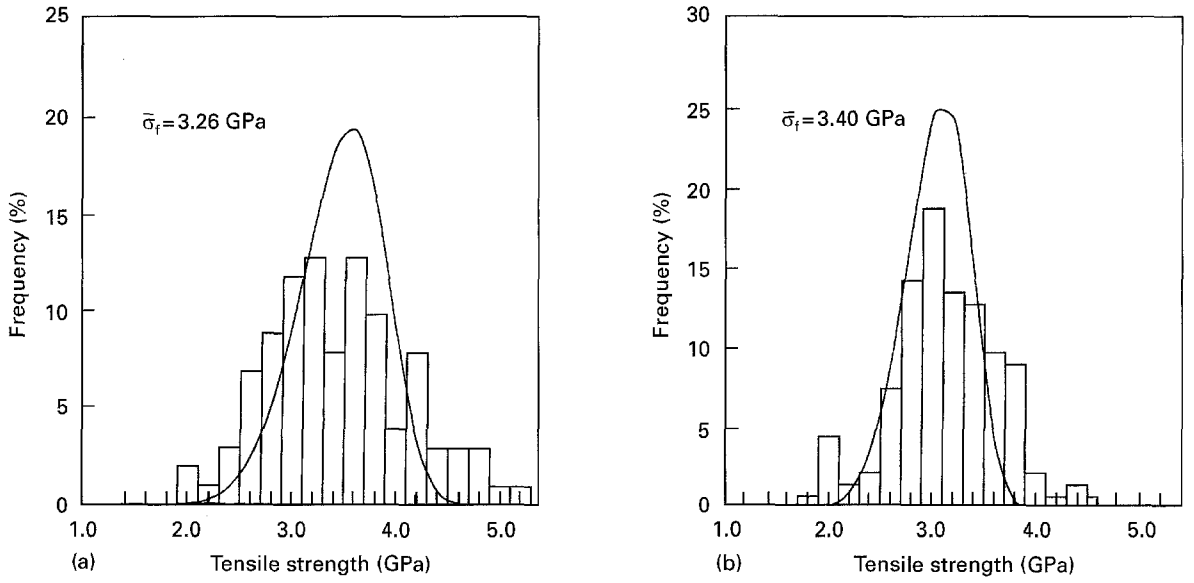

Figure 1 Strength distribution of fibres III. (a) Test length: 25 mm. (b) Test length: 100 mm. Refer to Table I for the sample symbols.

epoxy resin (Epikote 828, Yuka Shell) and 10 parts amine type curing agent (S-Cure 661, Kayaku Nuri) were mixed. This mixture was agitated thoroughly and then defoamed. This mixture was poured into a mould holding a fibre under constant tension in the neighbourhood of the surface of the rectangular specimen and subjected to curing at 65 °C for 17 h.

The specimens prepared in this manner were measured for fragment length, i.e. each specimen was subjected to a tensile (or compressive) strain of 4% at a drop rate of the upper heads of 10 mm min^{-1} using the four-bending method under the same conditions as reported in previous papers [6–11]. In this experiment, to investigate the effect of a radial compression force on the fibre axial compressive strength, measurements were made at 40–100 °C. Over 200 fragments were examined for each experimental condition.

3. Results and discussion

The typical strength distributions of graphitized fibres used in this experiment are shown in Figs 1 and 2.

The tensile strength of brittle fibres such as carbon fibres is generally affected by partial flaws. In general, the tensile strength of such fibres is represented by a chain model. This model represents a fibre with a chain consisting of n pieces of equal links. Applying the Weibull distribution function, probability $g(\sigma)$ in which a chain of n links will break at stress σ can be expressed as [12, 13]:

$$g(\sigma) = nm\sigma_0^{-1}\left(\frac{\sigma - \sigma_p}{\sigma_0}\right)^{m-1} \exp\left\{-n\left(\frac{\sigma - \sigma_p}{\sigma_0}\right)^m\right\} \quad (1)$$

where m, σ_0 and σ_p are the Weibull parameters. Also, the mean tensile strength $(\bar{\sigma}_{f,l})_t$ of the fibre at length L is given as [12, 13]:

$$(\bar{\sigma}_{f,l})_t = \sigma_p + \left(\frac{\sigma_0}{(L/l_l)^{1/m}}\right)\Gamma\left(\frac{m+1}{m}\right) \quad (2)$$

where Γ is the complete gamma function. l_l is the length of the link (gauge length L/number of links) consisting of the fibres.

The solid lines in Figs 1 and 2 represent theoretical values obtained by substituting Weibull parameters m, σ_0 and σ_p and the length l_l of links given in Table II into Equation 1.

The relationship between the logarithm of the gauge length and the logarithm of the mean tensile strength is also shown in Fig. 3. The solid lines in Fig. 3 represent theoretical values calculated by substituting Weibull parameters and the length of the links into

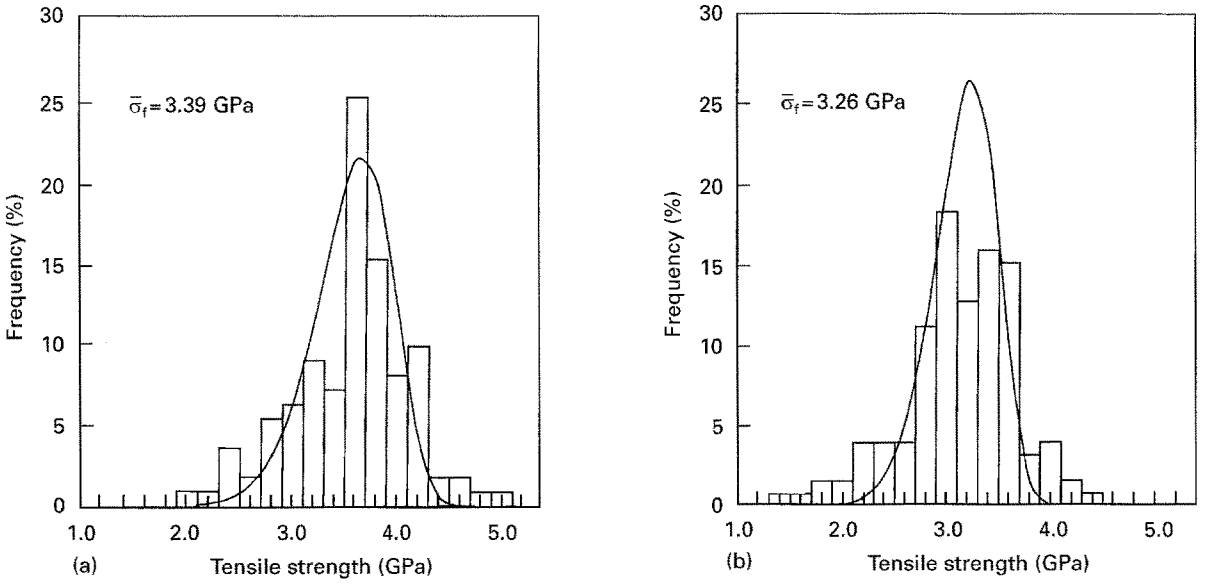

Figure 2 Strength distribution of fibres V. (a) Test length: 25 mm. (b) Test length: 100 mm. Refer to Table I for the sample symbols.

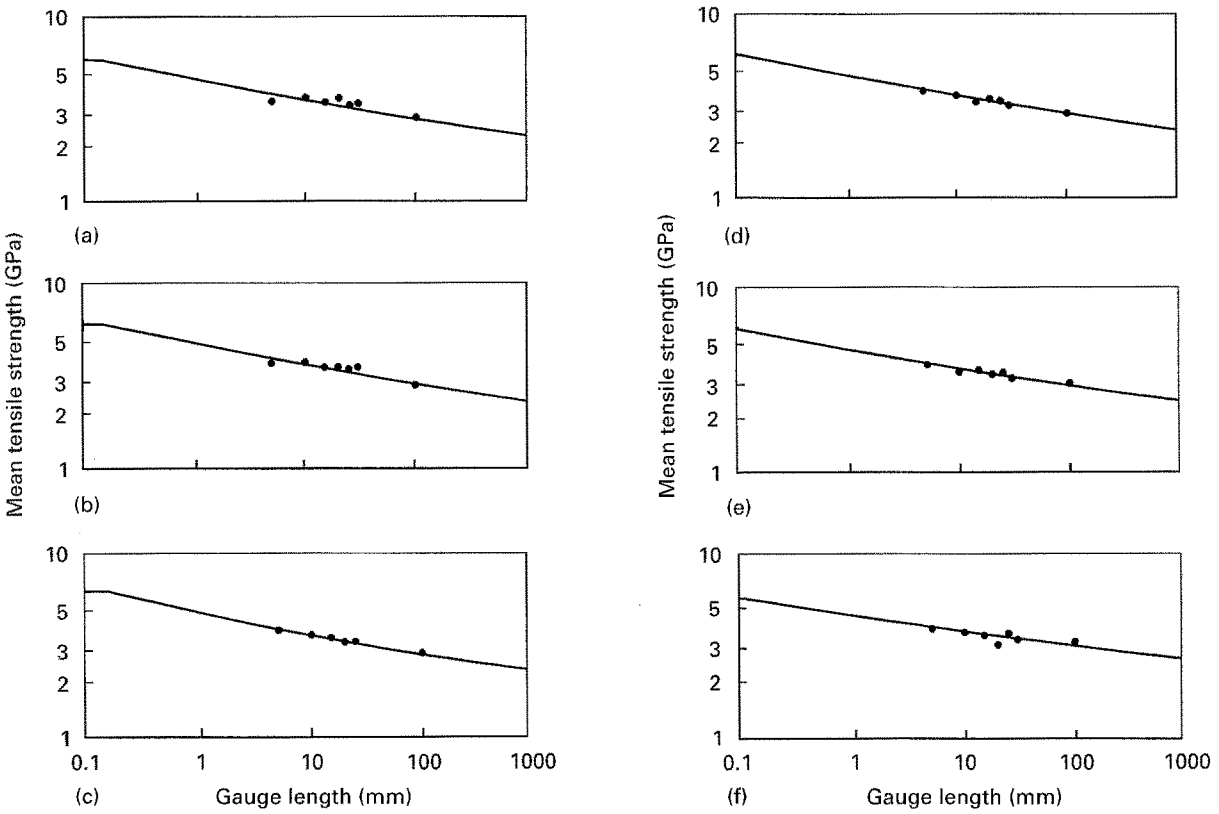

Figure 3 Relation between test length and tensile strength. (a) Fibre I; (b) fibre II; (c) fibre III; (d) fibre IV; (e) fibre V; (f) fibre VI. Refer to Table I for the sample symbols.

Equation 2. The theoretical values obtained by Equations 1 and 2, employing the values of Weibull parameters and the length of the links given in Table II, agree with the measured values. Therefore, the values of the Weibull parameters and the length of the links thus determined are valid. Moreover, the constant value of the mean tensile strength within the shorter gauge length range in Fig. 3 shows that the tensile strength of the fibre is uniform in the length range shorter than the link length.

TABLE II Statistical values of tensile strength for fibres

Fibre	m	σ_0 (GPa)	σ_p (GPa)	Length of links l_1 (mm)
I	6.5	5.48	1.17	0.080
II	6.7	5.57	1.02	0.125
III	5.1	5.50	1.47	0.125
IV	7.1	6.24	1.02	0.040
V	7.1	5.24	1.10	0.100
VI	7.8	4.85	1.19	0.100

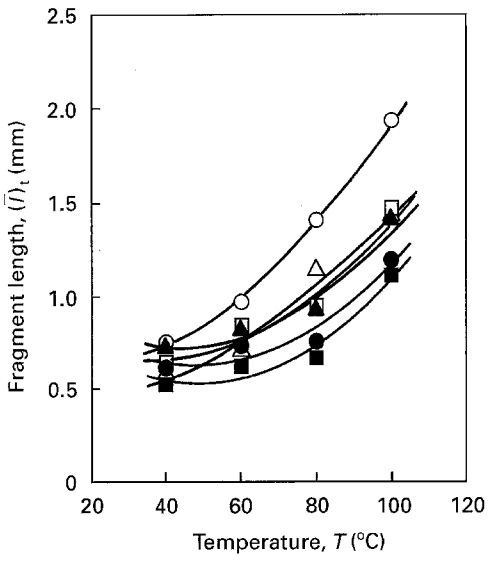

Figure 4 Relation between temperature and mean fragment length in tension. ○ Fibre I; △ fibre II; □ fibre III; ● fibre IV; ▲ fibre V; ■ fibre VI. Refer to Table I for the sample symbols.

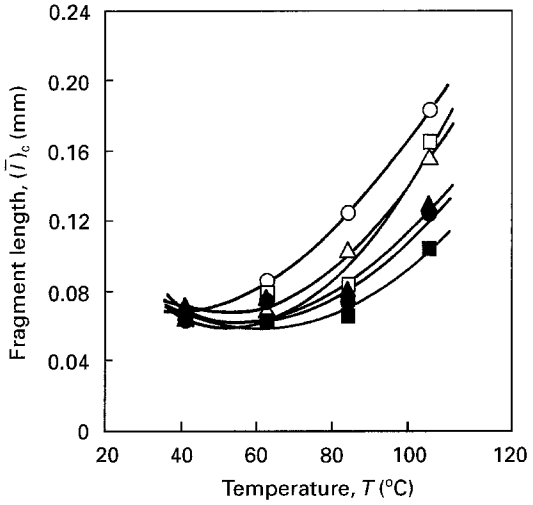

Figure 5 Relation between temperature and mean fragment length in compression. ○ Fibre I; △ fibre II; □ fibre III; ● fibre IV; ▲ fibre V; ■ fibre VI. Refer to Table I for the sample symbols.

In previous papers [8, 9], when the variable tensile strength of the fibre is assumed, the mean axial compressive strength $(\bar{\sigma}_f)_c$ of a fibre is given by:

$$(\bar{\sigma}_f)_c = (\bar{\sigma}_{f,l})_t \frac{(\bar{l})_c}{(\bar{l})_t} \quad (3)$$

where $(\bar{\sigma}_{f,l})_t$ is the mean tensile strength of the fibre at length L and is given by the above-mentioned Equation 2, $(\bar{l})_c$ is the mean fragment length in compression, and $(\bar{l})_t$ is the mean fragment length in tension.

The relationship between both mean fragment length $(\bar{l})_t$ in tension and $(\bar{l})_c$ in compression of composite systems including reinforcing fibres having tensile strength distributions and temperature are shown in Figs 4 and 5, respectively.

When all the fragments have been reduced to less than the critical fibre length, any further elongation of the specimen will not cause the fibre to break. When the fibre finally breaks into many pieces, we previously proposed that this considerable tensile strength was the tensile strength at the length just before the final fragment lengths [13].

If $\bar{l}$ represents the average value of the final fragment length, $K\bar{l}$ the first embedded length, and $k\bar{l}$ the length just before the length $\bar{l}$, then, the average value $\bar{L}^*$ of the length just before the fragment length with $\bar{l}$ is given by [13]:

$$\bar{L}^* = \frac{4}{3}\bar{l} + \sum_{k=3}^{K-1} k\bar{l}\frac{4}{k-1}\left(\frac{1}{3}\right)^{k-1} + K\bar{l}\frac{2}{K-1}\left(\frac{1}{3}\right)^{K-2} \quad (4)$$

The average value $\bar{L}^*$ of the length just before the length $(\bar{l})_t$ from the mean fragment length $(\bar{l})_t$ (Fig. 4) in tension according to Equation 4 can also be calculated. Furthermore, the mean tensile strength $(\bar{\sigma}_{f,l})_t$ of the fibres is determined by substituting the value into Equation 2 using the method described in previous papers [8, 9, 13].

Fig. 6 shows the relationship between the mean value of fibre axial compressive strength $(\bar{\sigma}_f)_c$ estimated from the mean fragment length $(\bar{l})_t$ (Fig. 4) in tension, the mean fragment length $(\bar{l})_c$ (Fig. 5) in compression, and the mean tensile strength $(\bar{\sigma}_{f,l})_t$ of the fibre according to Equation 3, and temperature. With these systems, in the same manner as observed in the carbon and aramid fibres [6–11], the estimated compressive strength decreases with increasing temperature up to 80 °C. As indicated elsewhere [6–11], it is conceivable that the radial force compressing the fibre, decreased by both the decrease in residual thermal stress and Young's modulus of the resin matrix with increasing temperature, may cause a temperature dependence of the estimated value of the fibre axial compressive strength.

The estimated compressive strength increases greatly above 80 °C. It is conceivable that the fibre buckles, and the conditions for application of the

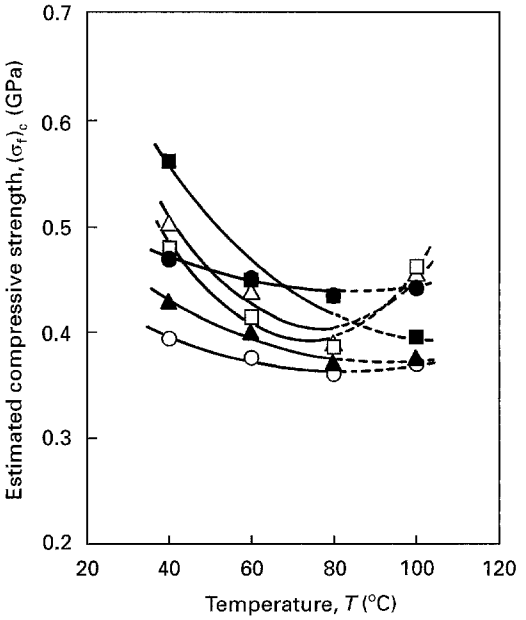

Figure 6 Relation between temperature and estimated mean compressive strength of the fibre. ○ Fibre I; △ fibre II; □ fibre III; ● fibre IV; ▲ fibre V; ■ fibre VI. Refer to Table I for the sample symbols.

TABLE III Thermal stress

Temperature (°C)	Thermal stress (MPa)
20	4.25
40	2.47
60	0.52
65	0

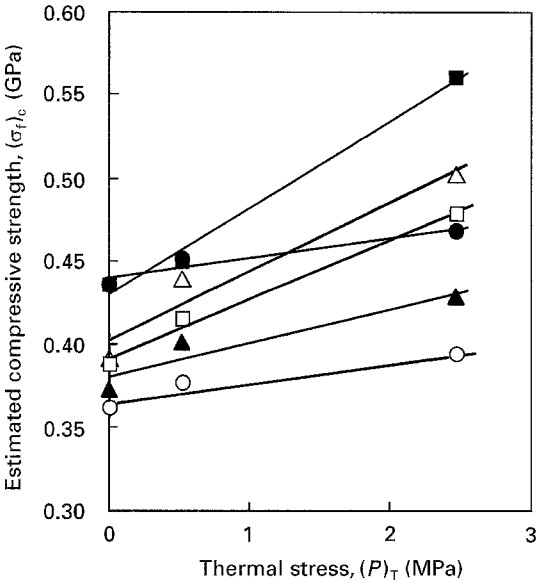

Figure 7 Relation between thermal stress and estimated mean compressive strength of the fibre. ○ Fibre I; △ fibre II; □ fibre III; ● fibre IV; ▲ fibre V; ■ fibre VI. Refer to Table I for the sample symbols.

above-mentioned Equation 3 cannot be satisfied above 80 °C [6–11]. Accordingly, further details are discussed for results obtained at a temperature range lower than 80 °C.

When a fibre is embedded in the resin and the system is allowed to cure, the thermal stress $(P)_T$ working perpendicularly on the fibre–resin interface is approximately given by the following equation [14]:

$$(P)_T = \frac{(\alpha_m - \alpha_f) E_m \Delta T}{1 + \upsilon_m} \quad (5)$$

where α is the thermal expansion coefficient, E is Young's modulus, ν is Poisson's ratio, ΔT is the difference in temperature from moulding temperature, and the subscripts m and f denote matrix and fibre, respectively. The thermal expansion coefficient α_m, Young's modulus E_m, and Possion's ratio ν_m required to calculate thermal stress were measured. The thermal stress $(P)_T$ was then calculated by Equation 5 as in a previous paper [11]. The thermal stress $(P)_t$ calculated from Equation 5 is shown in Table III. We have utilized a thermal expansion coefficient α_f perpendicular to the fibre axis, where α_f is $9.9 \times 10^{-6}\,°C^{-1}$ [15] for graphitized fibres. In addition, we have assumed that these values were constant in the temperature range of this experiment.

Fig. 7 shows the relationship between the estimated mean compressive strength $(\bar{\sigma}_f)_c$ (Fig. 6) and thermal stress $(P)_T$ (Table III) obtained through the function of temperature. With these fibres, the estimated mean compressive strength of graphitized fibres decreases linearly with decreasing thermal stress.

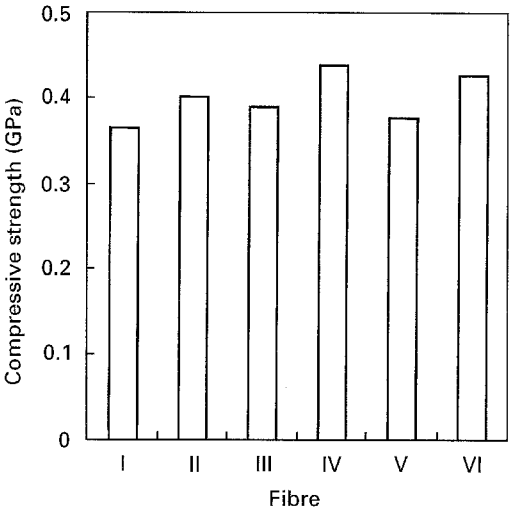

Figure 8 Compressive strength of the fibre with various surface- and/or sizing-treatments. Refer to Table I for the sample symbols.

As indicated in previous papers [6–11], it is conceivable that the real compressive strength of the fibres is the strength when the radial compression force, i.e. the residual thermal stress in this experiment, is zero. Accordingly, we have considered the value obtained by extrapolating the straight line in Fig. 7 to $(P)_T = 0$ as the real compressive strength of graphitized fibres. These real values of the fibres at various treatments are shown in Fig. 8. In comparison with the compressive strength of untreated fibre, its value for surface- or size-treated fibres is higher. Also, the surface-treatment is more effective than the size-treatments. In the case of size-treatment, the estimated compressive strength of fibre treated with ethylene oxide agrees approximately with that of fibre treated with epoxy oligomer. But, using epoxy oligomer as the sizing agent is more effective, as shown in Fig. 7, because the wettability with the resin matrix is better, therefore, as mentioned later, the shear yield strength at the fibre–matrix interphase is larger. Consequently, when the fibre is surface- and epoxy oligomer size-treated, it can be confirmed that the maximum compressive strength of the fibre is obtained.

As reported in previous papers [12, 13], by measuring the length of the broken fibre pieces, the shear yield strength τ at the fibre–matrix interface can be estimated by the following equation if it is assumed that the tensile strength of the fibre is variable:

$$\tau = \frac{(\bar{\sigma}_{f,})_t d}{2(\bar{l}_c)_t} \quad (6)$$

where d is fibre diameter, $(\bar{\sigma}_{f,})_t$ is the mean tensile strength of the fibre at length L and is given by the above-mentioned Equation 2. $(\bar{l}_c)_t$ is the mean critical fibre length in tension and is given by obtaining the mean fragment length $(\bar{l})_t$ in tension [12, 13]:

$$(\bar{l}_c)_t = \frac{4}{3}(\bar{l})_t \quad (7)$$

The average value $\bar{L}^*$ of the length just before the length $(\bar{l})_t$ can also be calculated from the mean fragment length $(\bar{l})_t$ (Fig. 4) in tension according to

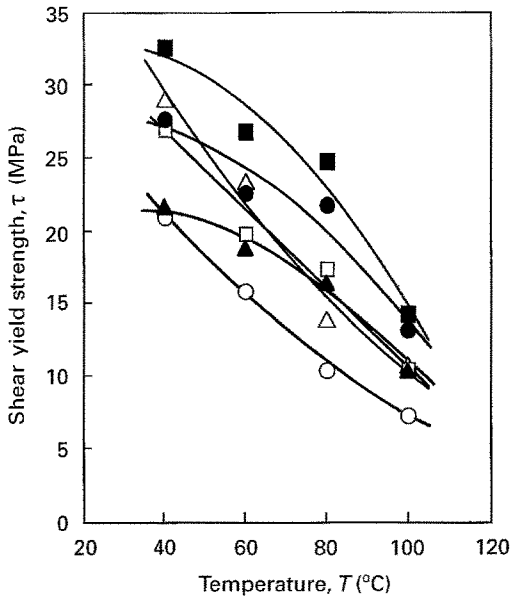

Figure 9 Relation between temperature and shear yield strength at the fibre–matrix interphase. ○ Fibre I; △ fibre II; □ fibre III; ● fibre IV; ▲ fibre V; ■ fibre VI. Refer to Table I for the sample symbols.

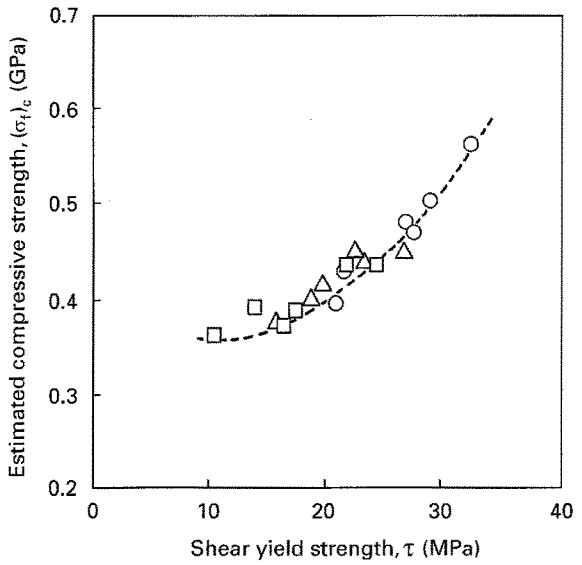

Figure 10 Relation between shear yield strength and estimated compressive strength of the fibre. ○ 40 °C; △ 60 °C; □ 80 °C.

Equation 4. Furthermore, the mean tensile strength $(\bar{\sigma}_{f,t})_t$ of fibres is determined by substituting the value into Equation 2 using a method described in previous papers [8, 9, 13] and is substituted into Equation 6. Also, the mean critical fibre length $(\bar{l}_c)_t$ in tension obtained from Equation 7 by substituting the mean fragment length $(\bar{l})_t$ (Fig. 4) in tension is substituted into Equation 6. The shear yield strengths τ at the fibre–matrix interphase are shown in Fig. 9.

Fig. 10 shows the relationship between the estimated mean compressive strength $(\bar{\sigma}_f)_c$ (Fig. 6) and the shear yield strength τ (Fig. 9) obtained through the function of temperature. With these surface- and/or size-treated fibres, the estimated mean compressive strength decreases with decreasing shear yield strength at the fibre–matrix interface and converges at about 0.35 GPa. Accordingly, it is found that the raw compressive strength of a fibre without surface- or size-treatments is about 0.35 GPa. As shown in Fig. 6, near room temperature, the effect of surface- and size-treatment on the axial compressive strength of the fibres is remarkable. Therefore, in order to obtain fibres with a higher compressive strength, the fibres should be surface- and size-treated.

4. Conclusions

If a sufficiently long fibre is embedded in the neighbourhood of the surface of a rectangular beam, and the system is subjected to a tensile (or compressive) strain greater than the fibre ultimate strain according to the bending method, the fibre eventually breaks into many pieces. By measuring the lengths of the broken pieces and estimating the mean tensile strength from the length just before the final fragment length in tension, attempts have been made to estimate the fibre axial compressive strength of pitch-based graphitized fibres, and the effects of surface- and size-treatment on compressive strength was investigated.

The estimated compressive strength of fibres decreases with increasing temperature. This decrease in compressive strength may be accounted for by a decrease in the radial compression force owing to a decrease in the residual thermal stress and a decrease in Young's modulus of the resin matrix.

There is a linear relationship between the estimated compressive strength and radial compression force in the temperature range from room temperature to 80 °C. The real compressive strength of the fibres, determined by extrapolating this straight line until the radial compression force is zero, increases with increasing shear yield strength at the fibre–matrix interphase. In order to obtain reinforcing fibres with a higher compressive strength, it will be necessary to surface- and size-treat the fibres.

By taking into consideration previous results [6, 7, 9–11], it was found that a fibre with higher compressive strength can be developed by increasing the degree of orientation or face spacing of the crystal, by decreasing crystal size, by decreasing fibre diameter, and by surface- and size-treatments.

Acknowledgements

We thank the Carbon Fibre Project Group, Corporate Research and Development Laboratory, Tonen Co., Ltd. for its financial contribution and the supply of the carbon fibres. Thanks are also due to Mr J. Takayasu, and Mr E. Tsushima for useful comments and discussions.

References

1. D. SINCLAIR, *J. Appl. Phys.*, **21** (1950) 380.
2. W. C. DALE and E. BAER, *J. Mater. Sci.* **9** (1974) 369.
3. J. H. GREENWOOD and P. G. ROSE, *ibid.* **9** (1974) 1809.
4. S. J. DETERESA, S. R. ALLEN, R. J. FARRIS and R. S. PORTER, *ibid.* **19** (1984) 57.
5. S. R. ALLEN, *ibid.* **22** (1987) 853.
6. M. MIWA, T. OHSAWA, M. KAWADE and E. TSUSHIMA, *Reinforced Plastics Jpn* **35** (1989) 199.

7. T. OHSAWA, M. MIWA, M. KAWADE and E. TSUSHIMA, *J. Appl. Polym. Sci.* **39** (1990) 1733.
8. M. MIWA, A. TAKENO and Y. LIU, *Reinforced Plastics Jpn* **37** (1991) 289.
9. M. MIWA, E. TSUSHIMA and J. TAKAYASU, *J. Appl. Polym. Sci.* **43** (1991) 1467.
10. M. MIWA, A. TAKENO, Y. LIU, A. WATANABE, J. TAKAYASU and E. TSUSHIMA, *Reinforced Plastics Jpn* **38** (1992) 433.
11. M. MIWA, Y. LIU, H. TSUZUKI, A. TAKENO and A. WATANABE, *J. Mater. Sci.* **31** (1996) 499.
12. M. MIWA, T. OHSAWA and K. TAHARA, *J. Appl. Polym. Sci.* **35** (1978) 795.
13. M. MIWA, T. OHSAWA and A. TOMITA, *Koubunshi Ronbunshu* **41** (1984) 353.
14. G. GERARD and A. C. GILLBERT, *J. Appl. Mech. (ASTM)* **24** (1957) 355.
15. A. KOBAYASHI, in 20th Air-Plane Symposium Japan (1982) p. 70.

Received 6 March
and accepted 1 December 1995